

METEOROLOGICAL CONDITIONS LEADING TO THE SAHARAN DUST EVENTS OBSERVED IN SOUTH FLORIDA IN JULY 2012

Nathan New¹ and Jeral Estupiñán^{2,*}

¹*Division of Meteorology and Physical Oceanography, Rosenstiel School of Marine and Atmospheric Science, University of Miami*

²*Miami Weather Forecast Office, National Weather Service, NOAA, Miami, FL*

ABSTRACT

This study focuses on six separate dust events from the month of July 2012 that reached Miami, FL. Using backward trajectories, the time and location of the dust lifting from near the surface were found as well as the meteorological conditions for the surface, 850mb, and 600mb levels. This process allowed for the relationship between time the dust spent aloft and origin location and the strength of the dust measured in Aerosol Optical Depth. The meteorological conditions of the entire month of July 2012 were examined against climatological averages in an effort to find a signal for the numerous dust events. Finally the daily averaged conditions were analyzed to find the transport mechanism for the dust to reach South Florida, as well as a comparison of the subtropical ridge during periods of activity during the month and a prolonged period of inactivity. Saharan dust has well documented effects on people's health and the ecosystem (Tobías et al. 2008; Walsh and Steidinger 2001). However, the effects of dust on precipitation and local weather (e.g. thunderstorms, cloud cover, etc) are not completely clear (Susan et al. 2009; Zhao et al. 2011; Albrecht 1989) and are active areas of research.

We found that neither the time the dust was aloft nor the origin of the dust was necessarily indicative of the strength when the dust reached Miami. Dust lifting occurred in two major locations: One on the Libya/Algeria border, and another in Niger, with Event 2 outlying in western Mauritania. Nigerien events all similar in strength (0.325 to 0.375 AOD), but the far North African origins ranged from the strongest to weakest events. It was also found that the 850mb chart best represented dust travel, and each event followed a ridge extending into the periphery of the subtropical high. The orientation of the subtropical ridge was found to be crucial for transporting dust to South Florida, with southerly and westerly maxima and an East-West elongation of the ridge most conducive for transport. The fastest movements of dust across the Atlantic came from westward expansion of the high causing a moving reference frame for the ridge carrying the dust. Forecasters at the Miami forecast office can use the results presented on this paper to increase the situational awareness during the summer months concerning Saharan dust events. This is expected to increase the accuracy of dust forecasting in South Florida.

**Corresponding author address:* Jeral Estupiñán,
Miami Weather Forecast Office, National Weather
Service, 11691 SW 17th Street, Miami, FL 33165; e-
mail: jeral.estupinan@noaa.gov

1.0 INTRODUCTION

1.1. Properties and Characteristics of Saharan Dust Outbreaks

Saharan dust is commonly found in the atmosphere throughout the year. The effects of Saharan dust on human health as well as the environment has been an area of active research (Tobías et al. 2008; Walsh and Steidinger 2001). This dust tends to originate from around 15°-20°N over north Africa, especially the Bodélé Depression (Chiapello et al. 1995; Chiapello et al. 1997; Touré et al. 2012). In this region, strong winds at the surface allow the dust to lift into the air where it encounters convection that lifts it even higher into the atmosphere. Dry and moist convection over the Saharan Desert allows for the mixed layer to reach as high as 500 millibars (mb) (Karyampudi and Carlson 1988). This mixed layer allows for a near even concentration of dust from the surface to this top at around 500 mb.

The dust moves westward along the trade winds as this mixing occurs. Once the dust reaches the Atlantic ocean, it becomes separated from the cooler Atlantic air near the surface due to fallout in the low levels. This elevated layer that transports the dust is known as the Saharan Air Layer (SAL) (Carlson and Prospero 1971). This SAL is bounded above at around 500 mb and the base normally lies within 850 mb to 900 mb (Ott et al. 1991). A column containing the SAL tends to be very stable. The air below the dusty region is relatively cool since it contains the boundary layer over the Atlantic. Potential temperature increases of 5-10 K are common from this boundary layer into the SAL (Karyampudi and Carlson 1988). The upper boundary of the SAL marks an increase in relative humidity allowing for a greater equivalent potential temperature than the dusty region maintaining this edge, though it is much less pronounced than the lower boundary (Carlson and Prospero 1971).

The SAL typically has a nearly constant potential temperature with a relatively low relative humidity compared to the surrounding air (Carlson and Prospero 1971). This region also tends to be drier than the surrounding due to stability decreasing the moisture flux from the Atlantic (Sun 2009); however, Huang et al. found that only 9% of dust outbreaks qualified as significant dry air outbreaks (2009). Therefore these events are dry within the layer, but moisture and clouds can persist above or below the dust. The increase in dust concentration also leads to an increase in Aerosol Optical Depth (AOD), allowing for detection of dust events through lidar and satellite. Estupiñan et al. (2012) noted that AOD of around 0.15-0.20 is detectable by the naked eye as being hazy and seemingly dusty in Miami.

1.2 Dust Origins

Chiapello et al. describe dust originating from two main sources in Africa (1997). They describe one origin as the Sahel just south of the Saharan Desert. This location is explained to be loaded within ridge extending from a surface high pressure over southern Europe and the Italian peninsula. The secondary common location of dust loading is explained to be the northwest Sahara. Dust from this region is typically loaded through a trough the winds caused by the heat trough over the African continent interacting with the Azores High. This second origin of dust is more common in the summer, when dust affects South Florida. Doherty et al. describe dust loading being caused by movements within the Azores high which impact the circulation of the tropics in the North Atlantic which enhance the easterlies over the North Africa (2008).

1.3. Transport of Saharan Dust

Though Saharan dust can be found at any time, the most likely period for it to be

transported across the Atlantic is between May and October (Carlson and Prospero 1974; Chiapello et al. 1995; Huang et al. 2009). These months show the furthest northward trajectories of dust parcels due to the northward shift of the Intertropical Convergence Zone and the onset of the West African Monsoon (Chiapello et al. 1995). During the boreal winter and spring, dust events do not move as far across the Atlantic, and those that do reach the western portion of the basin do so in South America (Huang et al. 2009). The journey for the SAL is difficult during the winter due to the shallow trade wind inversion with counter-trades above found during this time (Chiapello et al. 1995).

SAL dust outbreaks tend to follow along with African Easterly Waves (AEW) as they become more active during the summer months (Karyampudi and Carlson 1988). Within an AEW, the dust is likely to be bounded by two trough axes, and tends to be found on the east side of the major trough axis of the easterly wave. Within these waves, dust parcels tend to advance with respect to the lead trough axis allowing for it to possibly lie on the western side of the axis by the time the SAL reaches North America (Ott et al. 1991). Because of the dependence on easterly waves, the movement and period of dust events during the summer follows that of these easterly waves, moving at around 1000 km day^{-1} and with a period of near a week (Huang et al. 2009). Huang et al. also note that only around half of the dust events that move across the Atlantic retain the characteristics of the SAL. The rest either deposit enough dust to lose significance or are diminished by other forcings (2009).

1.4. Effects of Dust on Weather

The effect of Saharan dust on the weather of the tropical Atlantic has been the focus of recent research. The effect this dust has on tropical cyclones has received the most

attention as the summer months see both dust events and tropical cyclones. Though there have been studies on the effects of dust on tropical cyclones, whether dust benefits or detracts tropical cyclones is still being debated. The SAL helps create a mid level easterly jet due to the thermal wind profile of the hot dusty layer compared to the cooler maritime air surrounding it. This jet helps bring vorticity to the tropical Atlantic as well as creating beneficial ageostrophic lifting on the equator side (Karyampudi and Carlson 1988; Shu and Wu 2009). However, the dust itself can change the microphysics, hydrometeor processes, diabatic heating profile, and thermodynamics of the atmosphere, such that it is difficult to determine the benefits or detracts on intensification (Zhang et al. 2007). The shear caused by the thermal wind profile of the layer is one undoubtable detriment to tropical cyclone intensification, while other factors are more debatable (Dunion and Velden 2004).

The effects of dust on daily weather like that found in South Florida during the summer has not seen the same level of research as the effects on tropical cyclones. Zhao et al. found that dust events do have effects on precipitation in the African monsoon. They noted that the SAL absorbs shortwave radiation during the day due to the properties of the dust particles. At night, the SAL emits this energy in the longwave spectrum in all directions. Some of that energy is emitted towards the surface causing it to warm in comparison to a non dusty night. This warming helps destabilize the low levels allowing for enhanced precipitation at night (Zhao et al. 2011). Dust can also affect the strength and number of updrafts leading to generally more updrafts during dust outbreaks (Susan et al. 2009). Though there are more updrafts, the presence of so many cloud condensation nuclei (CCN) means that rainfall is not as heavy during thunderstorms as drops are less likely to coalesce with so many CCN

(Susan et al. 2009). Due to this inhibition of rainfall, cloud and thunderstorm lifetime can be extended with the added concentration of dust (Albrecht 1989), yet the extent of this process is not well known (Rosenfeld and Feingold 2003).

1.5. July 2012 Events

During the month of July 2012, Maimi saw six distinct dust events (Estupiñan et al.

2012). The July events can be seen in Figure 1. These events were defined by having a daily averaged AOD greater than 0.20, and were verified using a visual basis. Multiple consecutive days meeting this criteria were classified as the same dust event as they likely had the same origins. Estupiñan et al. found that dust outbreak days averaged an AOD of 0.333 compared to 0.182 during clean days (2012).

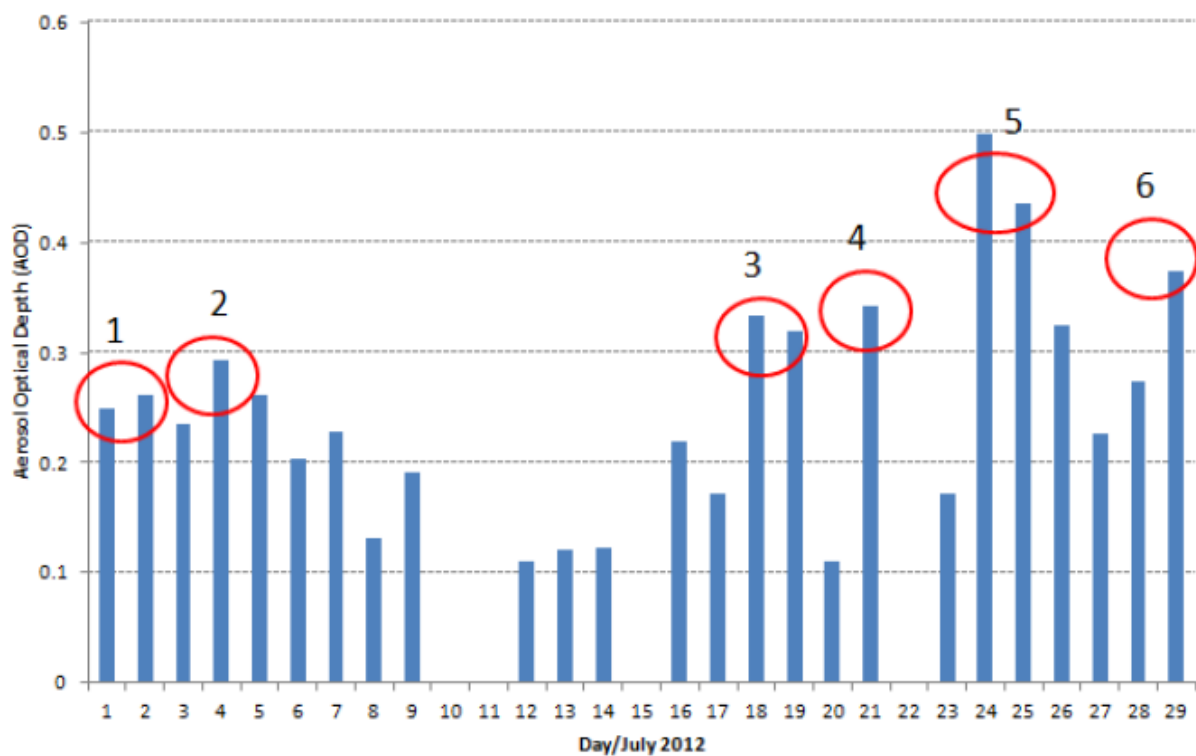


Figure 1: Dust events in July 2012 numbered as Events 1-6 (Estupinan et al. 2012).

2.0.DATA

2.1 Lidar

The University of Miami operates a Sigma micro pulse lidar atop its Rosenstiel School of Marine and Atmospheric Science campus on Virginia Key in the Biscayne Bay east of Miami. This lidar transmits at 532nm with a one minute time resolution and 75 meter vertical resolution alternating between a co-polarized and cross-polarized phase to discriminate between aerosol and cloud. The university uses this data to create a product displaying intensity and the depolarization

ratio from 0-3km as well as 0-15km. Since the dusty layers regularly exceeded 3km in height, the 0-15km product was used (Rosenstiel School of Marine and Atmospheric Science 2013). This product determined when during the days of each event the dust concentration began, peaked, and ended based on the intensity measurement of the lidar in the low levels as seen in Figure 2. The low levels of the top image of Figure 1 showing yellows and oranges depict areas of higher intensity returns and the presence of aerosols.

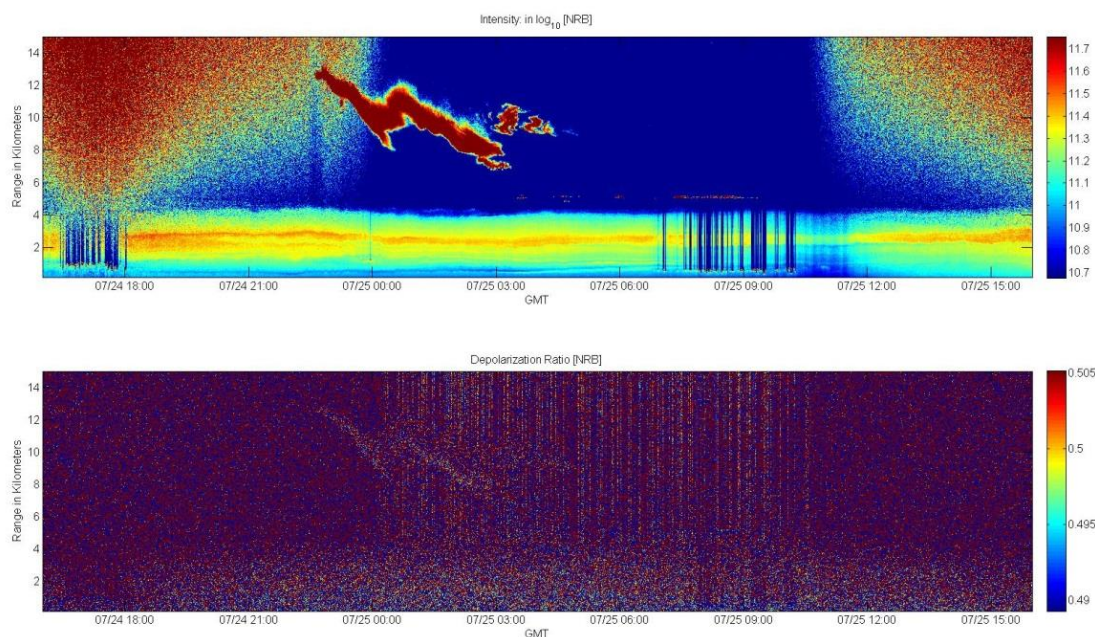


Figure 3: Lidar image from July 24, 2012 (Event 5) depicting the dry dusty layer from around 500 m to nearly 4000 m. Best seen through the deep yellows and oranges at around 2500 m.

2.2. *HYbrid Single-Particle Lagrangian Integrated Trajectory (HYSPLIT) Model*

The Air Resources Laboratory operates the HYSPLIT model to compute trajectories of air parcels. This model

incorporates meteorological reanalysis or forecast models as well as the starting time and location to compute forwards and backwards trajectories of air parcels at a given location and height (Draxler and

Rolph 2013; Rolph 2013). This model was run utilizing the archived GDAS1 analysis for a location centered at Miami International Airport. The vertical motions of the parcel were calculated through the model's vertical velocity and the model ran backwards the maximum time allowed of 315 hours at 500m elevation intervals.

2.3. NCEP/NCAR Reanalysis

The Earth Systems Research Laboratory operates the NCEP/NCAR Reanalysis1. This product operates on a global grid with 17 pressure levels. The temporal scale offers long term means from 1981-2010 as well as monthly, daily, and 4-times daily values from 1948 to the present. The Mean Sea Level Pressure (MSLP) as well as geopotential heights for various pressure

levels were gathered from this reanalysis.

3.0 METHODS

3.1 Tracing Dust Parcels

The dates for the 6 dust events from July 2012 were found by Estupiñan et al. using data from the Aerosol Robotic Network that measures daily averaged AOD from Key Biscayne, Florida (2012). Using the dates known from this previous work, the lidar data provided by the University of Miami was used to find times during each day as well as the height levels that best represent the dust parcels in the SAL. Lidar analysis found that the most representative parcels for the SAL and the dust contained within can be seen in Table 1.

Table 1: Date Time and Height for each event to be used in the HYSPLIT model.

Event	Date	Time	Height
1	1 July	1500 UTC	500 m - 1500 m
2	4 July	0000 UTC	1000 m
3	19 July	1800 UTC	2500 m
4	21 July	1500 UTC	2000 m
5	24 July	1800 UTC	2500 m
6	29 July	1200 UTC	1000 m – 2000 m

These times and heights were then imputed into the HYSPLIT model running a backwards trajectory from Miami International Airport for 315 hours, the maximum time allowed. For some events, 315 hours was not enough time to trace the SAL back to the origin location in Africa. When this happened an additional 315 hour run was initialized from a point and time along the path of the dust trajectory.

3.2 Verifying Dust Trajectory

In order to ensure the given trajectories reflected the actual phenomena of dust transport, a verification process was utilized for the trajectories of each event. The trajectories were used to find times and locations of the dust once it entered the domain of the Meteosat-9 satellite over Africa

and the eastern Atlantic. Then the Dry Air/Saharan Air Layer product from the Cooperative Institute for Meteorological Satellite Studies (CIMMS) (2013) was used to ensure the parcel trajectory was contained within the movement of the identified SAL. The SAL product only analyzes the dust over the ocean, as seen in Figure 2. To follow the parcels over the continent, a mid-level infrared (IR) satellite and water vapor (WV) imagery was used. The location of the parcel is found

with the trajectory and SAL product, then is followed backwards through features in the mid-level IR and WV over the continent to verify parcel movement to the initial loading location. Following this process, the trajectories from each event analyzed made meteorological sense when compared to satellite data, so each trajectory was accepted as a close representation of the truth for the events.

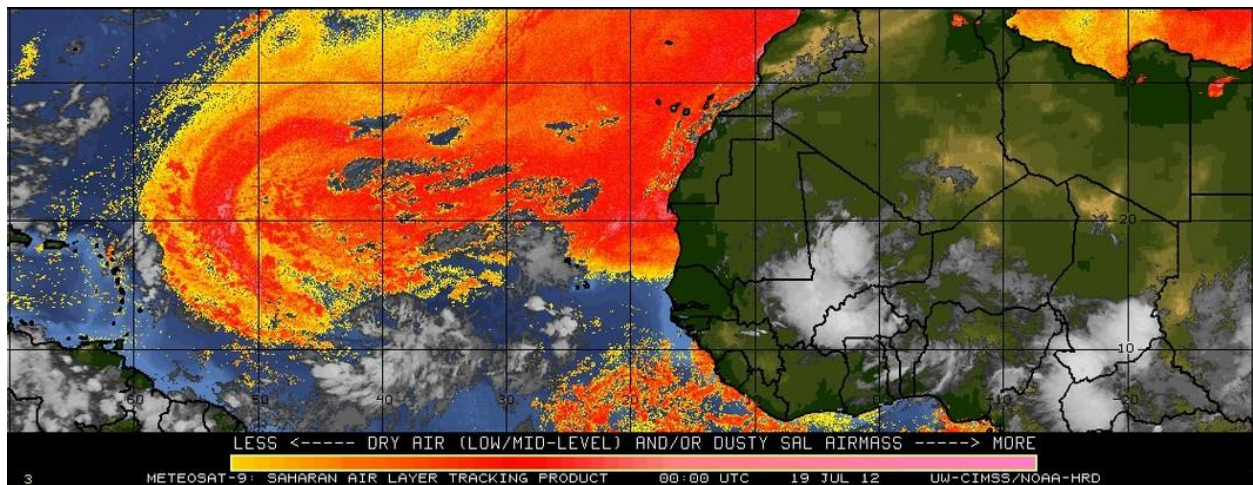


Figure 3: SAL image from CIMMS on 19 July showing dust (warm colors) ejecting from Africa across the Atlantic.

3.3 Meteorological Analysis

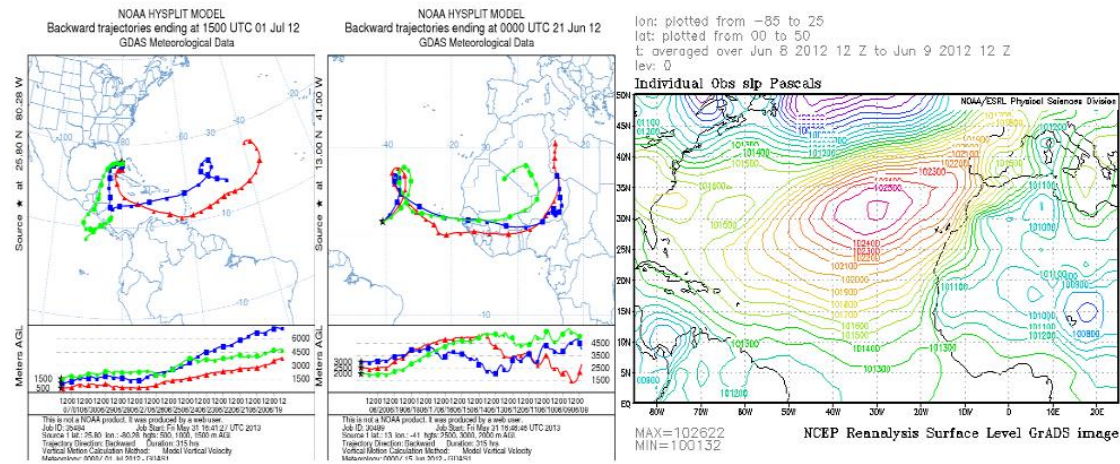
To find the meteorological conditions that led to the loading of dust, the surface maps from the time of loading as well as the IR and WV images were used. These plots were utilized in an attempt to find convection and updrafts that would loft the dust from the surface. They were also used to describe the flow regime and loading sector scheme laid out by Chiapello et al. (1997). Once the dust had been loaded, the 850 mb and 600 mb charts as well as the surface maps were analyzed for the Atlantic domain during the time the dust traveled across the Atlantic to South Florida.

4.0 RESULTS

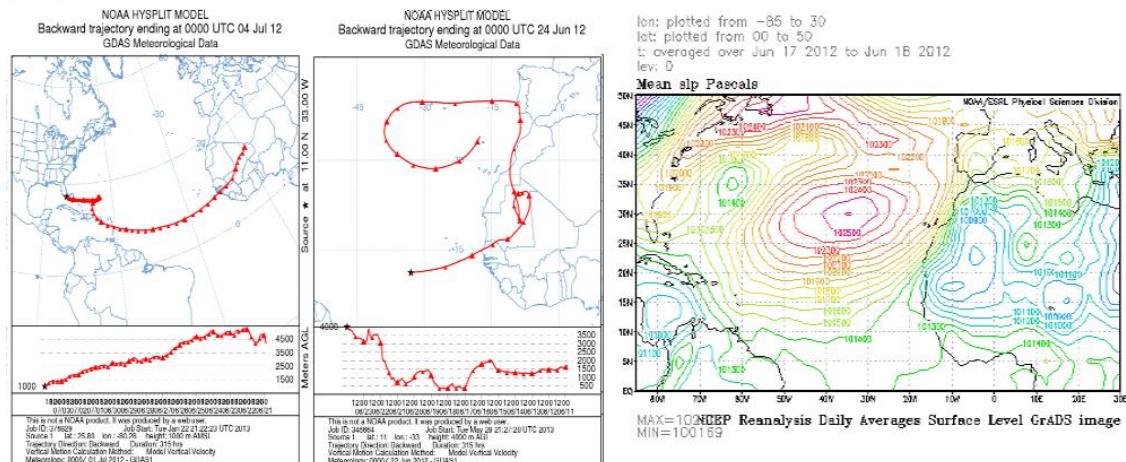
4.1 Parcel Tracing

Using the work done by Estupiñan et al. (2012) to identify the six events from the month of July 2012 seen in Figure 1 as well as lidar analysis from each event, the trajectories for each dust event were calculated. These trajectories can be found in Figures 4 and 5, with Figure 4 representing the trajectories of the first three events and Figure 5 showing the trajectories from the last three events. The second trace from each of the events using a point along the path of the original trace shows the likely loading location and times for each event. The trajectories

Event 1



Event 2



Event 3

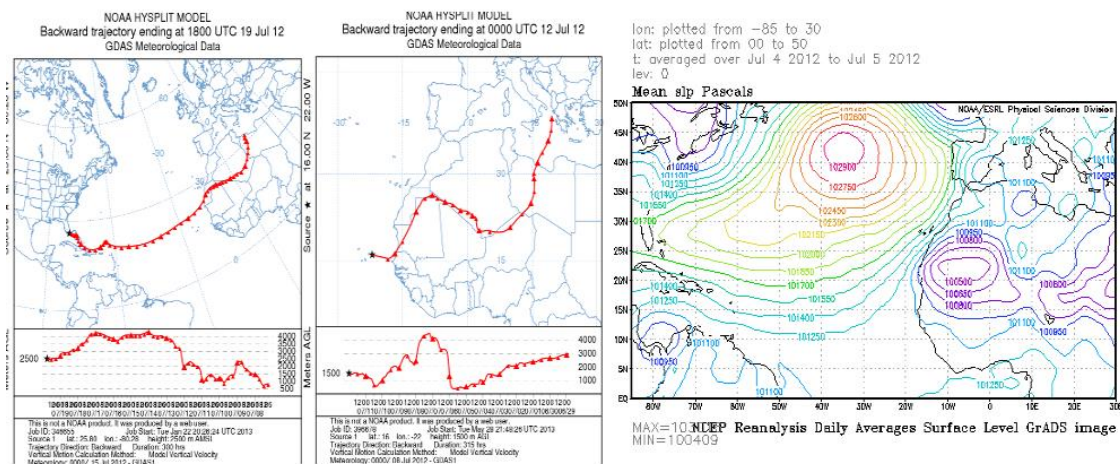


Figure 2: Trajectories for the first three events during July 2012 as well as the surface map displaying Mean Sea Level Pressure during the time the parcel lifted from its lowest level over Africa.

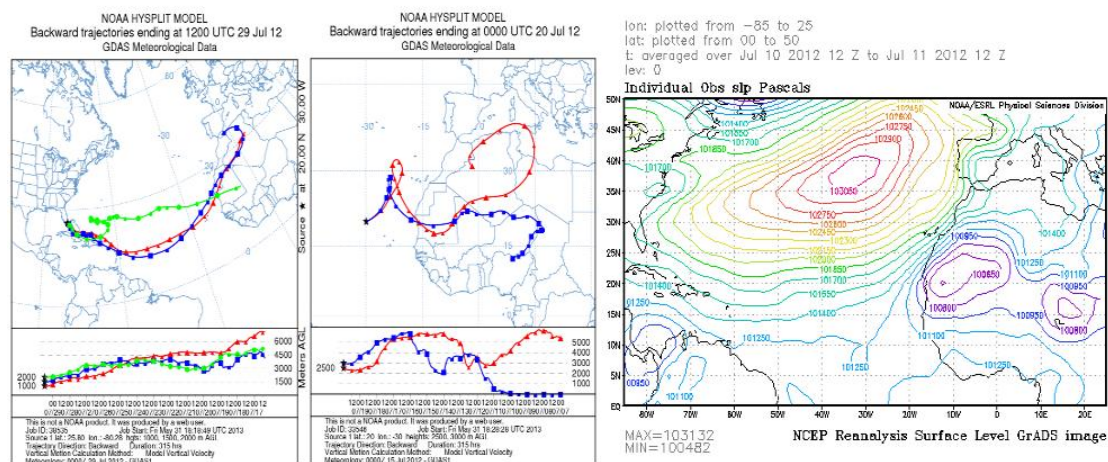
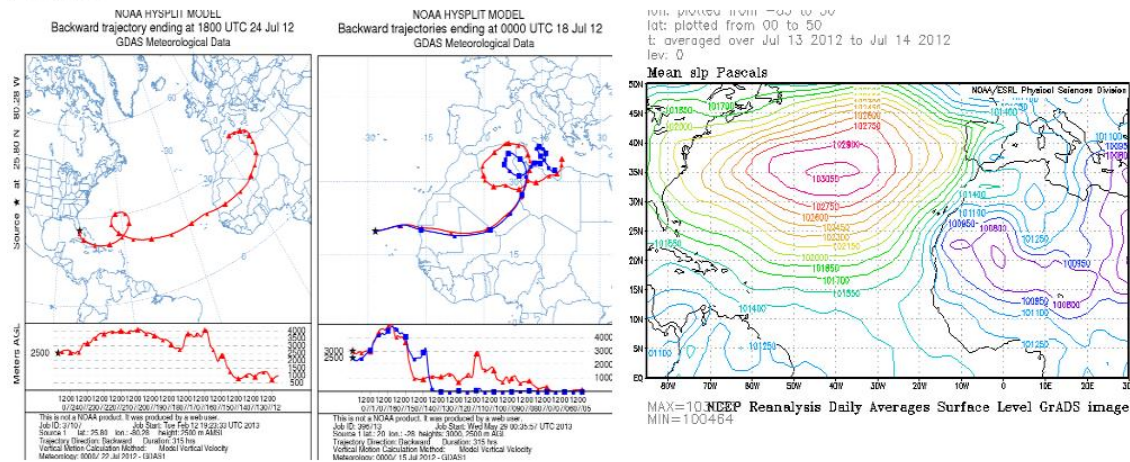
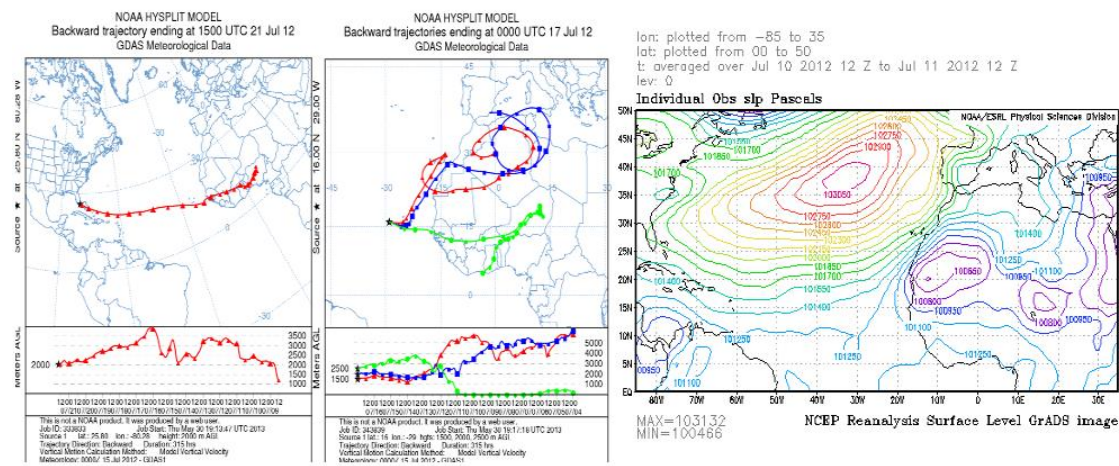


Figure 3: Trajectories for the last three events during July 2012 as well as the surface map displaying Mean Sea Level Pressure during the time of lifting from the parcel's lowest level over Africa.

showed the dust parcels at or very near the ground in five of the six events. Only Event 1 contained dust that was mixed into the layer at around 1500 meters above ground level. This event was also the weakest of the month, with the stronger AOD signatures representing parcels that were traced to the surface over North Africa. The surface conditions from Figures 3 and 4 during the time of dust loading allow for estimations at the origins of the dust using the regimes laid out by Chiapello et al. (1997). The surface conditions imply that Events 1, 4, 5, and 6 likely originated from North Africa, and Event 3 likely originating from the Sahel, while Event 2 does not follow either of the archetypical patterns.

These traces allowed for a calculation of the amount of time each event took to traverse the ocean. Events 1 and 6 took about the same amount of time to reach from loading to South Florida with around a 20 day journey, the longest of all the events. The second longest time was Event 2 having taken 16 days to reach the Miami area from loading. Event 3 was almost as long with 15 days. Finally Events 4 and 5 were the shortest periods of 10 days each. Using AOD as a representation of the strength of the dust event, Event 5 was the strongest of the month, followed by Event 6, Event 4, Event 3, Event 2, and Event 1 respectively. This means that

the time that the dust takes to travel across the ocean does not necessarily represent the strength of the event when it reaches South Florida. With dust falling out of the SAL into the ocean over time, intuition expects the longer a parcel remains over the Atlantic the weaker it would be. Since Event 6 took the longest time from loading to reaching Florida, this intuition would assume that the event would be weak, yet it was the second strongest event recorded during the month. This arrives at a limitation of the trajectory analysis. A certain parcel within the SAL may have been loaded at the time described by Event 6 in Figure 4 twenty days before reaching Florida. However, dust is constantly being loaded into the atmosphere during this time, as evidenced by Event 5 loading later than Event 6, keeping the layer dusty while over near the African continent.

These trajectories also allowed for the location of the origin of the dust from each event as seen in Figure 6. This figure was created from the location of the trajectory for each event when the model indicated lifting surface or lowest level. The figure shows that most of the locations of the lifting of the dust occurred just east of the prime meridian in Niger or along the Libya – Algeria border. Event 2 was an outlier with the dust originating from northern

Dust Origin by Location of Lifting

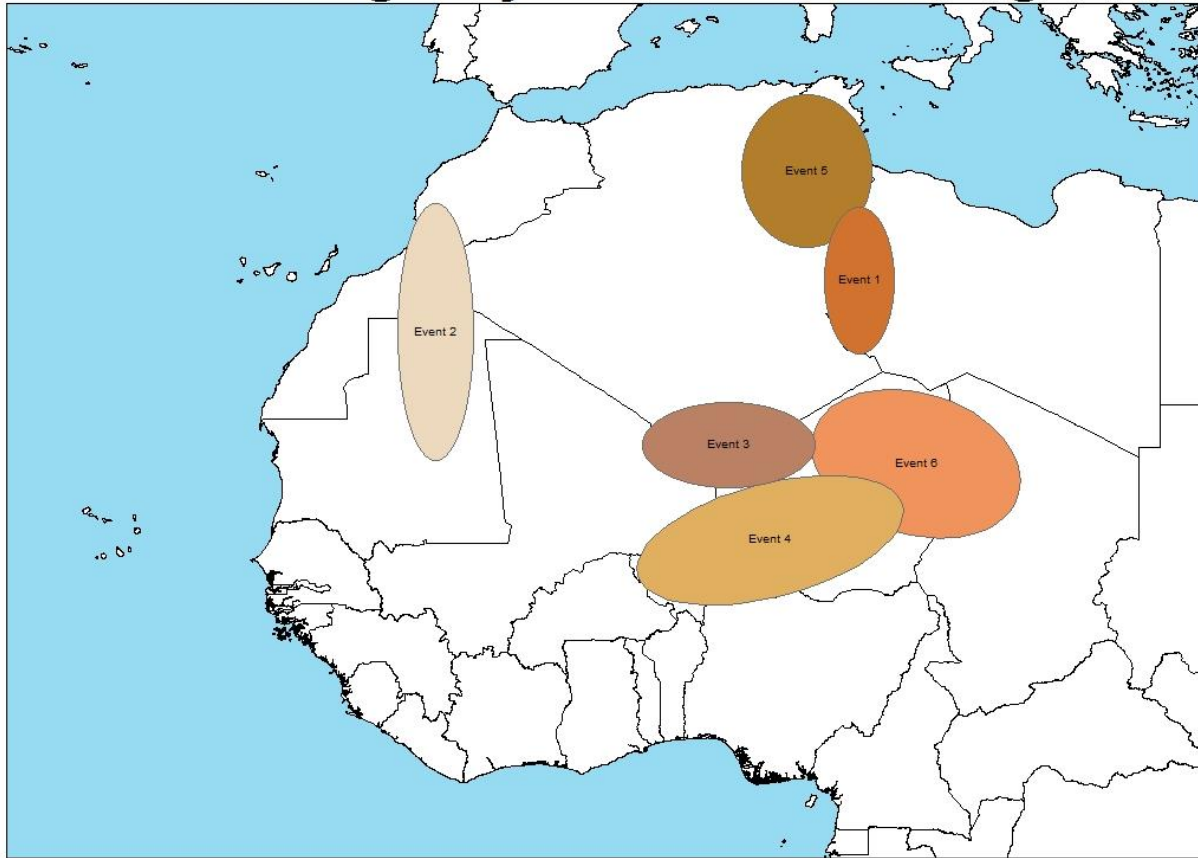


Figure 4: Location of likely dust loading based on the trajectories calculated through the HYSPLIT model.

Mauritania. The locations in the graphic follow fairly closely with the likely origins of dust laid out by Chiapello et al. (1997). Events 6 and 4 were expected to originate from further north by the flow regime, but the rest follow closely to what was expected earlier. This graphic also shows no trend in origin location with strength of the dust layer when it arrived to South Florida. The strongest event, Event 5, likely originated from Tunisia or East Algeria. This origin is just north of the likely loading point of the weakest event, Event 1. The events clustered in Niger however all had similar strengths when arriving to Florida. The strongest from this region, Event 6, registered just less than 0.4 AOD, while the weakest from the region, Event 3, registered near 0.35 AOD when it

reached South Florida. Because of the discrepancies between Events 6 and 1 originating in very similar locations, it can be concluded that the strength of the dust when reaching Florida is not solely a function of the location that the dust was loaded.

4.2 Meteorological Conditions

Since the dust originated from various locations over North Africa, the surface and upper level analyses were analyzed to find the transportation that caused the heightened activity during July 2012. The monthly mean Mean Sea Level Pressure (MSLP) chart in Figure 7 shows a maximum contour of 1028mb for the Azores High at 35N - 40N and 30W – 40W, and a

minimum

contour of 1007mb for the African heat low. In comparison, the long term July average MSLP map in Figure 8 shows a maximum of 1025mb for the Azores High from around 30N – 37N and 30W – 45W and a minimum 1008mb heat low. This means that July 2012 the subtropical ridge was centered further north and east on average than climatology, but the 1025mb contour in 2012 contained the average July 1025mb contour. The strength of the subtropical high and heat low were found for each year in the 1981-2010 period to compare 2012 to the variability within this time. It was found that the maximum contoured strength of the subtropical ridge found within the entire 31 years including 2012 was 1028mb. Highs this strong were found nearly a third of the time though at 10 of the 31 years. This strong of a high was also found in 2011, a year with comparatively few dust events over South Florida (Rosenstiel School of Marine and Atmospheric Science 2013), so the strength does not necessarily translate to more dust events. The minimum low found over Africa during this 1981-2010 period was contoured at 1006mb during 1995, with a slightly higher 1007mb contoured

during 2012. 1007mb or lower minimum contours were found in 10 of the 31 years as well, yet an average low that strong had not occurred since 2007.

To track dust parcels across the Atlantic, the HYSPLIT indicated location of the dust at certain times through the transportation process were plotted. Figure 9 shows a plot of the parcel in black for Event 1 over the surface map, 850mb map, and 600mb map. The charts were plotted at a period of nearly four days. Figure 9 indicates that the dust during this event follows within a ridge extending from the subtropical high at the surface and 850mb levels with a weaker signature at the 600mb level. Since the dust parcels are transported at a height ranging from 1500m to 3500m, the levels between 850mb and 600mb would likely represent the environmental conditions exerted on the dust since the height of these layers bound the range of the dust. As evidenced in Figure 9, the 850mb level shows a higher number of contours making analysis easier. This trend of ease in analyzing the 850mb chart extends into all the events, so the 850mb chart will be used for each event

lon: plotted from -90 to 25
lat: plotted from 00 to 50
t: Jul 2012
lev: 0

Mean slp millibars

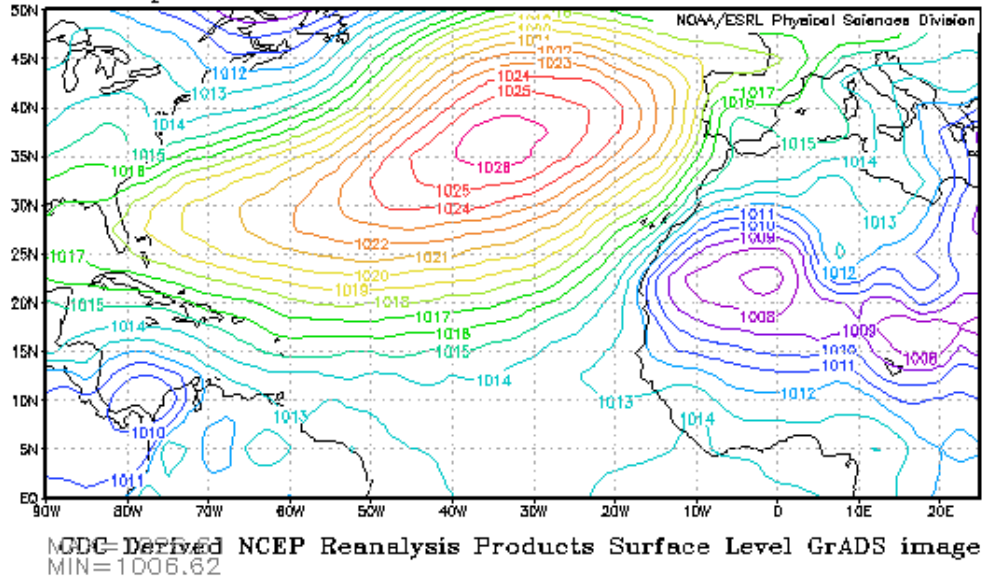


Figure 7: Monthly Average Sea Level Pressure for July 2012

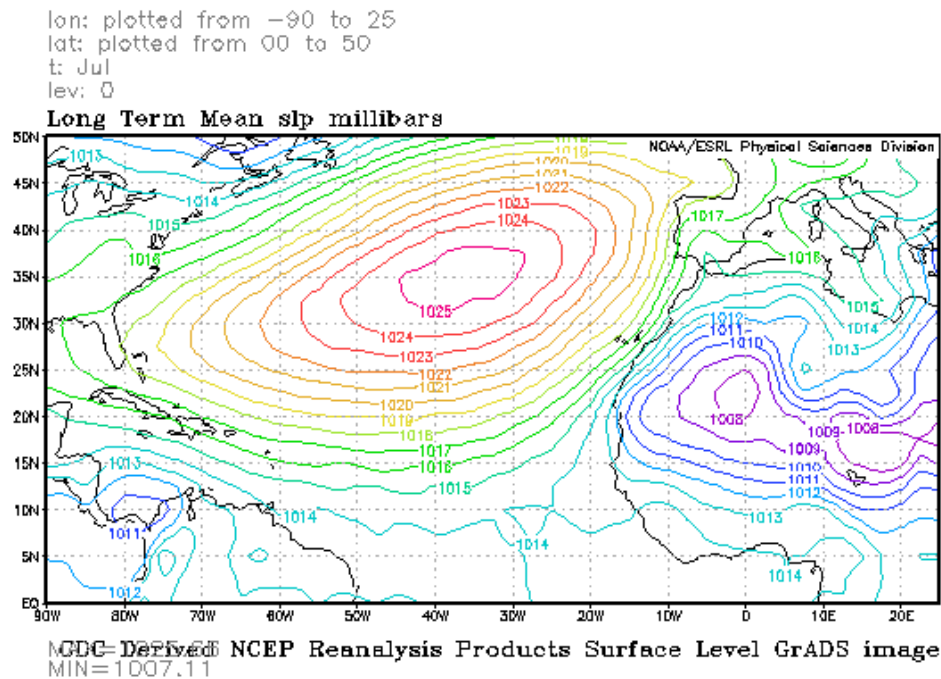


Figure 8: Long Term Monthly Average Mean Sea Level Pressure for July (1981-2010)

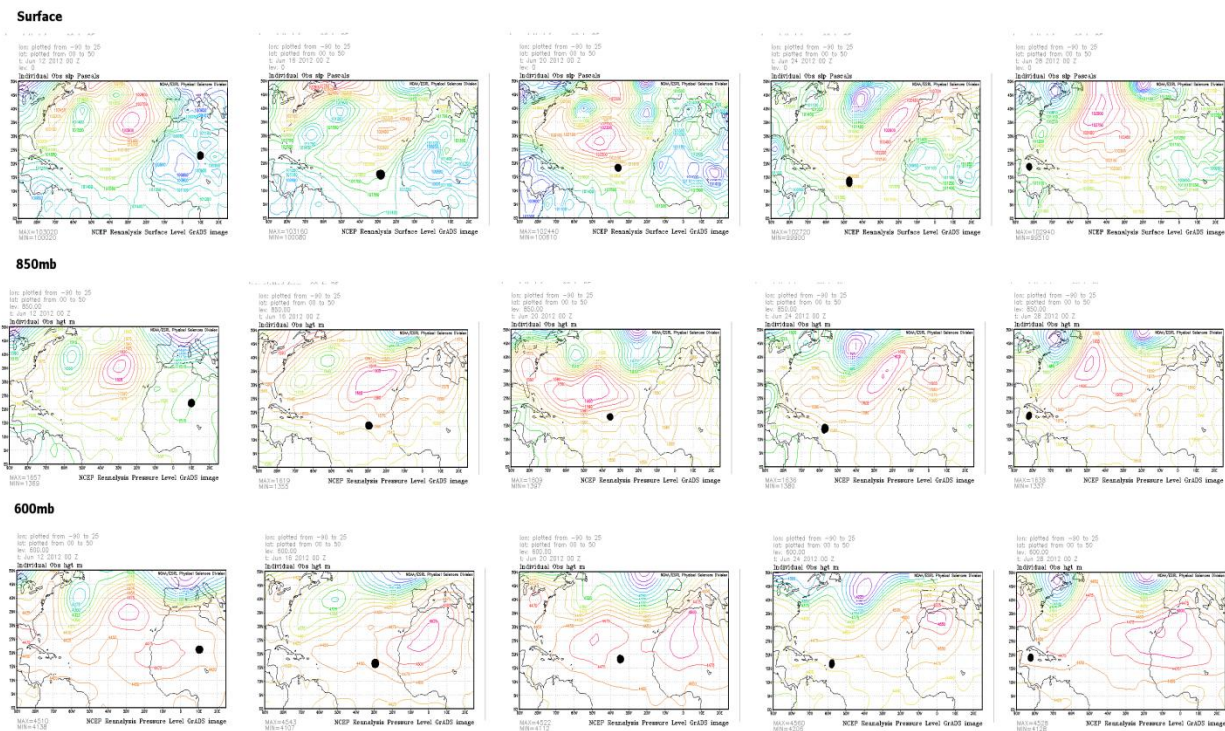


Figure 5: Location of model indicated dust (black) for surface, 850mb, and 600mb during transit across the Atlantic

Figure 10 shows the 850mb chart contours as well as the parcel location for the first three events of the month, with Figure 11 showing the latter three. These time steps between charts for each event vary based on the time the dust took to reach South Florida from lifting. Therefore, Events 4 and 5 have faster time steps of two days where Events 1 and 6 have longer time steps of 4 days. These graphics show that once the dust layer had lifted and moved to the coast of Africa, it was absorbed into a ridge in the periphery of the subtropical high. The movement of this ridge dictated the pace at which the dust moved from its loading location to South Florida. Event 3 also shows that until the dust was absorbed in a ridge feature, it remained nearly stationary over West Africa before moving very quickly across the entire Atlantic Ocean. These figures also show that a westward expansion of the subtropical high allow for much faster movements of the dust to North America. Event 5 shows how the dust moved more than 30 degrees west within a two day period while the high was expanded about 15 degrees west. Between the 20th and the 22nd, however, the subtropical high progressed back to the east causing the dust layer to remain nearly stationary in the western Atlantic before finally being pushed into South Florida by a strengthening high in the West Atlantic.

Lidar data for the entire month of July can be found in Figure 12. In this figure,

darker colors in the low levels of the top image show higher aerosol content and are indicative of African dust. This figure shows two periods of activity during the month; one during the first days, from July 1 to July 5, and another later in the month sporadically from July 19 to July 24, then persistently from July 24 to July 30. These two periods of activity were separated by a lull in dust transported from around July 5-6 to around July 16-17. Figure 13 shows the 850mb chart averaged from June 29 to July 4. This figure shows the average 850mb conditions during the first period of activity, as the events of early July began travelling in late June. The subtropical high was centered on 35N – 40N and 40W. The high was elongated into Florida, with contours to the south nearly zonal from the central Atlantic to the Greater Antilles. This ridge was expansive as well, with the 1550m contour from 15N over the Lesser Antilles to around 18 north of Jamaica. Figure 14 shows the 850mb chart from the second period of activity, averaged from July 17 to July 29. This figure shows a high centered further south between 30N – 35N and further west to around 45W. This ridge too elongated to the southeast with a ridge axis over southern Florida. The expanse was very similar to the first active period as well with the

1550m

Figure 10 displays 16 maps of NCEP Reanalysis Pressure Level Q1000 images, arranged in a 4x4 grid. The maps are organized into two rows of four, corresponding to Event 2 (top row) and Event 3 (bottom row). Each map shows the pressure level Q1000 contours and a black dot indicating the location of the event. The maps are titled with the event name and the time range of the data. The maps are arranged in two rows of four, with the top row for Event 2 and the bottom row for Event 3. Each map includes a title with the event name, a subtitle with the time range and data source, and a legend with the minimum value (Min).

Event 2

- Map 1: NCEP Reanalysis Pressure Level Q1000 image. Time range: -90 to 25. Data source: NCEP Reanalysis Pressure Level Q1000. Min: 1350.
- Map 2: NCEP Reanalysis Pressure Level Q1000 image. Time range: -90 to 25. Data source: NCEP Reanalysis Pressure Level Q1000. Min: 1352.
- Map 3: NCEP Reanalysis Pressure Level Q1000 image. Time range: -90 to 25. Data source: NCEP Reanalysis Pressure Level Q1000. Min: 1352.
- Map 4: NCEP Reanalysis Pressure Level Q1000 image. Time range: -90 to 25. Data source: NCEP Reanalysis Pressure Level Q1000. Min: 1350.

Event 3

- Map 5: NCEP Reanalysis Pressure Level Q1000 image. Time range: -90 to 25. Data source: NCEP Reanalysis Pressure Level Q1000. Min: 1350.
- Map 6: NCEP Reanalysis Pressure Level Q1000 image. Time range: -90 to 25. Data source: NCEP Reanalysis Pressure Level Q1000. Min: 1352.
- Map 7: NCEP Reanalysis Pressure Level Q1000 image. Time range: -90 to 25. Data source: NCEP Reanalysis Pressure Level Q1000. Min: 1352.
- Map 8: NCEP Reanalysis Pressure Level Q1000 image. Time range: -90 to 25. Data source: NCEP Reanalysis Pressure Level Q1000. Min: 1350.

Figure 6: 850mb chart with dust location (black dot) for the first three events of July 2012

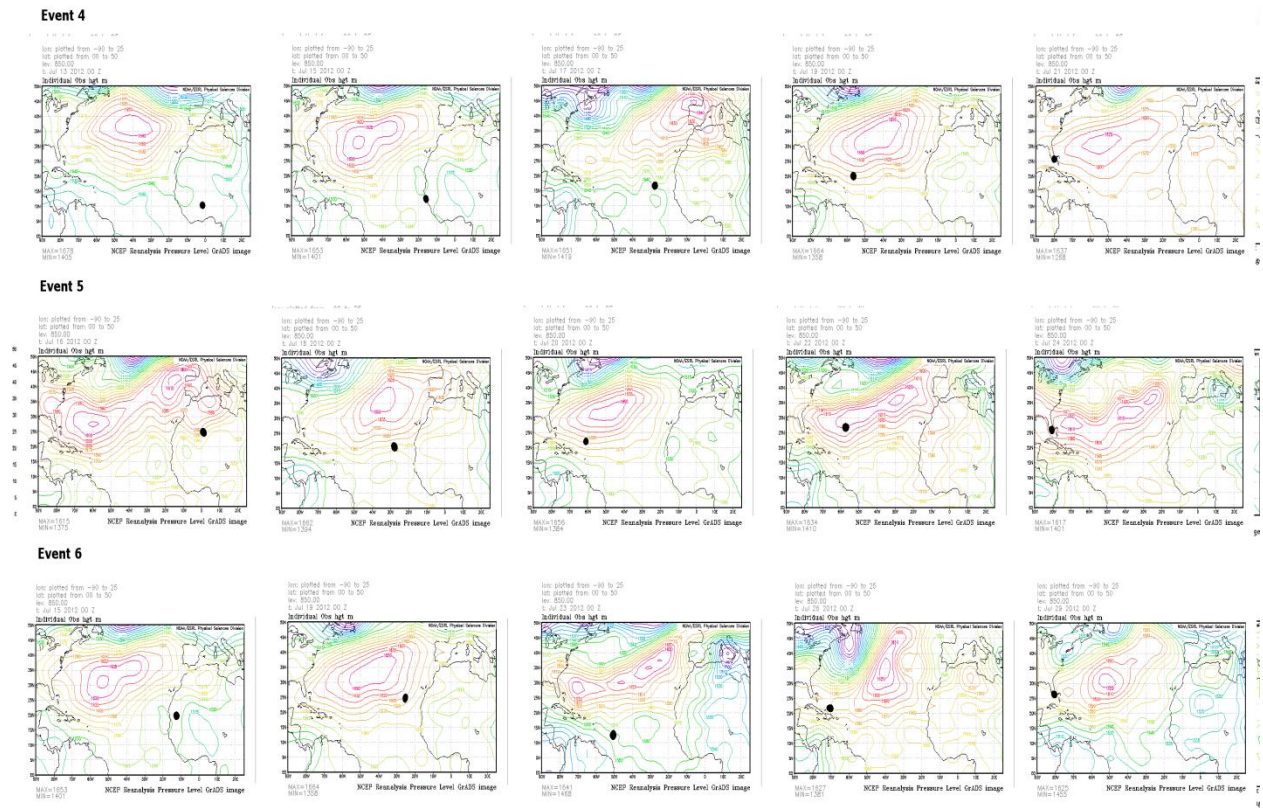


Figure 7: 850mb chart with dust location (black dot) for the last three events of July 2012

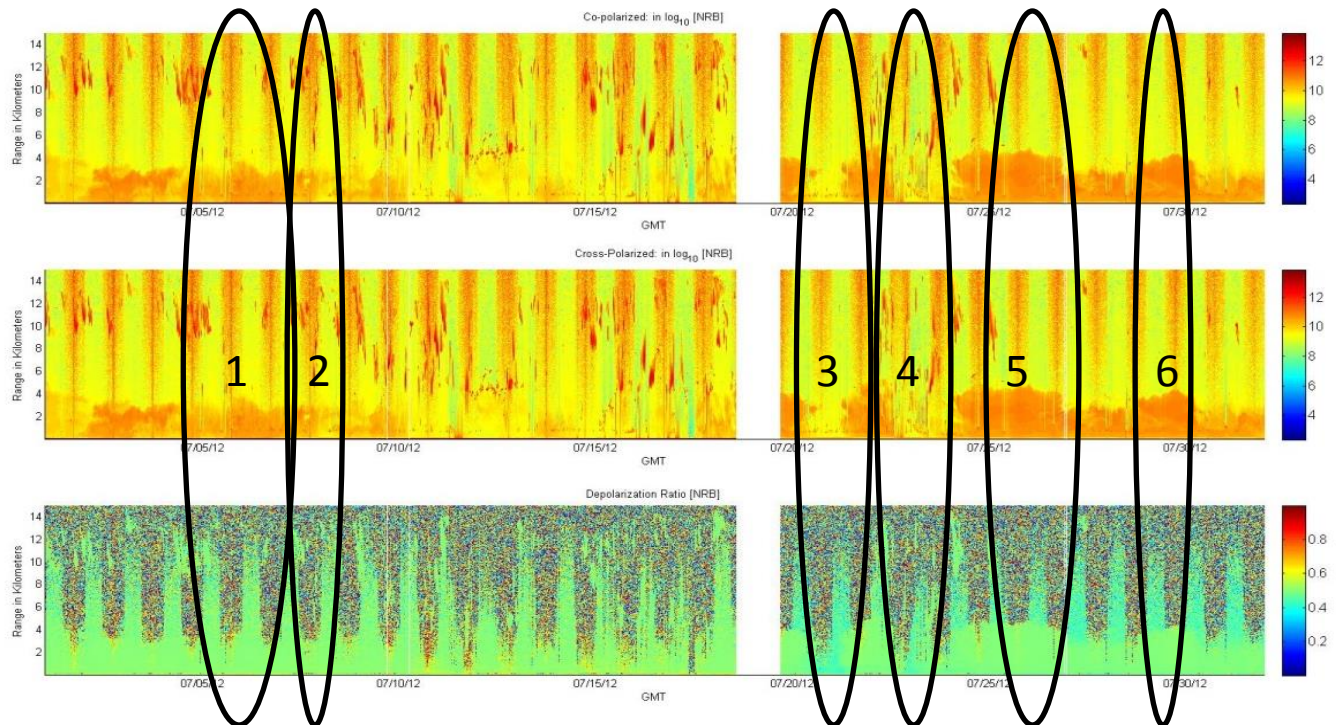


Figure 8: Lidar data for the month of July 2012 showing dust as darker colors in the lowest levels of the first two images with each event marked by an oval and a number corresponding to the event number

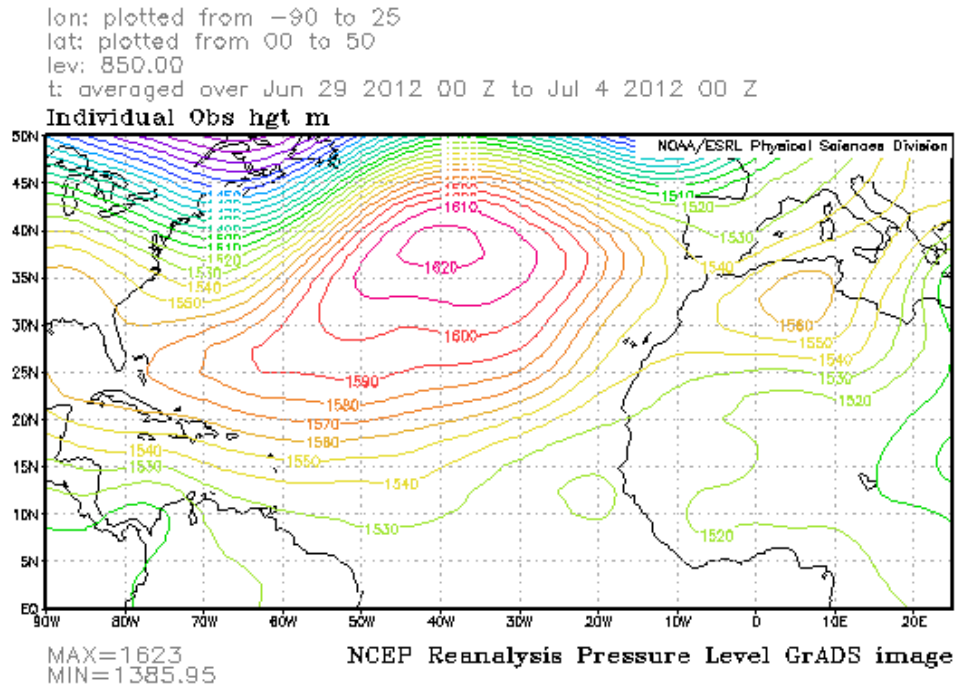


Figure 9: 850mb chart for June 29 to July 4, representing the time of dust transport for Events 1 and 2 and the first period of activity during the month

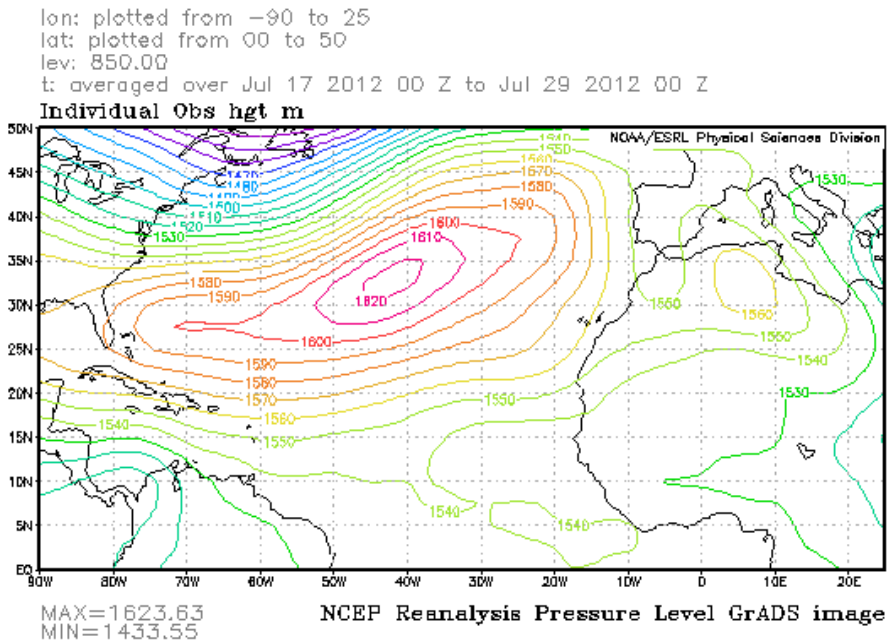


Figure 10: 850mb chart averaged from July 17 to July 29, the second active period for South Florida with the transportation of Events 3 – 5.

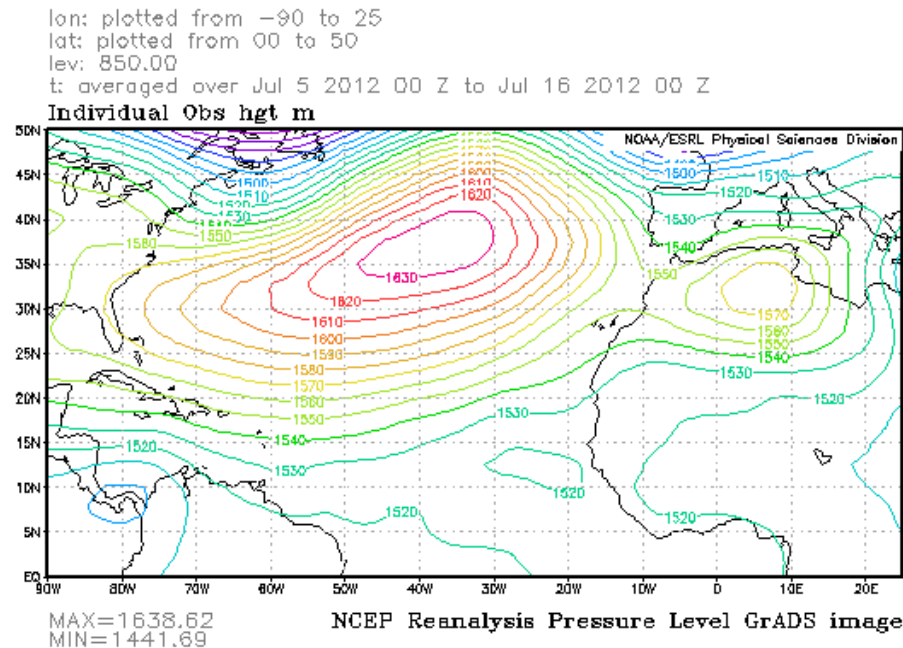


Figure 11: 850mb chart averaged from July 5 to July 16, a lull in dust activity for South Florida.

height contour located in the exact same place over the Caribbean Sea. The two shared a high of 1820m as well.

Figure 15 shows the same 850mb chart for the lull between the activity, from July 5 to July 16. This figure shows a slightly stronger high of 1830m located 35N – 40N and around 35W. This high was slightly further east than the two active periods, but the ridge elongation was much further north with an axis through southern Georgia while curving to the northwest over the east coast. The ridge is also slightly less expansive with the 1550m contour from around 18N north of the Lesser Antilles to 21N north of Jamaica. Due to the ridge axis extending to the south located further east of the active periods, as well as having stronger curvature, dust transported across the Atlantic would either dive into the Caribbean and not pull into Florida, or be curved to the north too soon to impact the Miami area causing the decreased activity during this time. The evidence of this lull

during the month helps explain that the movement of the subtropical ridge and the waves within leads to dust transport to different locations of the Atlantic.

5.0 CONCLUSIONS

Estupinan et al. found six Saharan dust events in Miami during the month of July 2012. Some of these events comprised of multiple days, and in all 12 days during the month recorded AOD of 0.25 or higher (2012). These events were analyzed through lidar data located on Virginia Key in the Biscayne Bay east of Miami, FL. Through lidar, the times that the dust reached a peak, as well as the height of the dust layer were obtained. These times and heights were then imputed into the HYSPLIT trajectory model to plot the path of the dust from its origins in Africa. With these plots, the location and time of the dust movement for each event was found, and a suite of surface and upper air plots were found. This allowed for a look at

the ambient conditions surrounding the dust layer and helped explain the activity for South Florida. The conclusions are as follows:

- The time taken for each dust event to reach South Florida from lifting was found.
 - Events 4 and 5 were 10 days each
 - Events 2 and 3 were 16 and 15 days respectively
 - Events 1 and 6 were each 20 days
- Event 5 was the strongest followed by Events 6, 4, 3, 2, and 1 in that order.
- The time the dust spent in the air did not determine the strength as evidenced by Event 6 taking the longest time to reach Florida yet still was the second strongest event.
- Dust lifting occurred in two major locations. One on the Libya – Algeria border, and another in Niger, with Event 2 outlying in western Mauritania.
- Nigerien events all similar in strength (0.325 to 0.375 AOD), but the far North African origins ranged from the strongest to weakest events.
- July 2012 averaged MLSP showed the subtropical high contoured at 1028mb for its maximum and the African heat low contoured at 1007mb for its minimum. Climatological (1981-2010) averages showed a maximum contour of 1025mb and a minimum contour of 1008mb.
- .
- Maxima contours of 1028mb for the subtropical high were found in 10 years of the period, and minima contours for the African heat low of 1007mb were also found in 10 separate years, but the two did not necessarily overlap meaning each occurs approximately a third of the time
- The 850mb chart best showed the dust movement when compared to the surface chart and the 600mb chart.
- Dust layers follow within ridges in the periphery of the subtropical high.
- The fastest movements of dust across the Atlantic came from westward expansion of the high causing a moving reference frame for the ridge carrying the dust.
- Two periods of activity during the month were split by a period of inactivity
- The average positions for the subtropical high in each of the two active periods was south and west of the inactive period, with a more zonal elongation and more zonal contours on the southern side.
- Forecasters at the Miami forecast office can use the results presented on this paper to increase the situational awareness during the summer months concerning Saharan dust events. This is expected to increase the accuracy of dust forecasting in South Florida

References

- Albrecht, B. A., 1989: Aerosols, cloud microphysics, and fractional cloudiness. *Science.*, **245**, 1227–1230.
- Carlson, Toby N., Joseph M. Prospero, 1972: The Large-Scale Movement of Saharan Air Outbreaks over the Northern Equatorial Atlantic. *J. Appl. Meteor.*, **11**, 283–297.
- Chiapello, I., et al, 1995: An Additional Low Layer Transport of Sahelian and Saharan Dust Over the North-Eastern Tropical Atlantic. *Geophys. Res. Lett.*, **22(23)**, 3191–3194.
- Chiapello, I., G. Bergametti, B. Chatenet, P. Bousquet, F. Dulac, and E. S. Soares, 1997: Origins of African dust transported over the northeastern tropical Atlantic, *J. Geophys. Res.*, **102(D12)**, 13701–13709.
- CIMSS, cited 2013: CIMSS Tropical Cyclones Data Archive Request. [Available online at tropic.ssec.wisc.edu/archive/]
- Doherty, O. M., N. Riemer, and S. Hameed, 2008: Saharan mineral dust transport into the Caribbean: Observed atmospheric controls and trends. *J. Geophys. Res.*, **113**.
- Draxler, R.R. and Rolph, G.D., 2013: HYSPLIT (HYbrid Single-Particle Lagrangian Integrated Trajectory) Model access via NOAA ARL READY Website (<http://ready.arl.noaa.gov/HYSPLIT.php>). NOAA Air Resources Laboratory, Silver Spring, MD.
- Dunion, Jason P., Christopher S. Velden, 2004: The Impact of the Saharan Air Layer on Atlantic Tropical Cyclone Activity. *Bull. Amer. Meteor. Soc.*, **85**, 353–365.
- Estupiñan, Jeral, Dan Gregoria, Kenneth J. Voss, Roberto Arias, 2012: Characteristics Of The Saharan Dust Events Observed in The Month of July, 2012 At Miami Florida: Aerosol Physical Characteristics And Vertical Distribution – Presentation, 2012 SPoRT / NWS Partners Virtual Workshop.
- Huang, Jinfeng, Chidong Zhang, Joseph M. Prospero, African dust outbreaks, 2010: A satellite perspective of temporal and spatial variability over the tropical Atlantic Ocean, *J. Geophys. Res.*, **115**.
- Kalnay et al., 1996: The NCEP/NCAR 40-year reanalysis project. *Bull. Amer. Meteor. Soc.*, **77**, 437–470.
- Karyampudi, V. Mohan, Toby N. Carlson, 1988: Analysis and Numerical Simulations of the Saharan Air Layer and Its Effect on Easterly Wave Disturbances. *J. Atmos. Sci.*, **45**, 3102–3136.
- Ott, S-T., A. Ott, D. W. Martin, J. A. Young, 1991: Analysis of a Trans-Atlantic Saharan Dust Outbreak Based on Satellite and GATE Data. *Mon. Wea. Rev.*, **119**, 1832–1850.
- Rolph, G.D., 2013: Real-time Environmental Applications and Display sYstem (READY) Website (<http://ready.arl.noaa.gov>). NOAA Air Resources Laboratory, Silver Spring, MD.
- Rosenfeld, D., and G. Feingold, 2003: Explanation of the discrepancies among satellite observations of the aerosol indirect effect. *Geophys. Res. Lett.*, **30**, 1776.
- Rosenstiel School of Marine and Atmospheric Science, cited 2013: CAROb micropulse lidar. [Available online at <http://carob.rsmas.miami.edu/mpl.html>]
- Shu, S., and L. Wu, 2009. “Analysis of the influence of Saharan air layer on tropical cyclone Intensity Using AIRS/AQUA data”. *Geophys. Res. Lett.*, **36**.
- Sun, D., W. K. M. L., Kafatos, M., Boybeyi, Z., Leptoukh, G., Yang, C., & Yang, R., 2009. Numerical simulations of the impacts of the saharan air layer on atlantic tropical cyclone

- development. *J. Climate*, **22(23)**, 6230-6250.
- Susan C. van den Heever, Gustavo G. Carrio, William R. Cotton, Paul. J. DeMott and Anthony J Prenni, 2009: Saharan dust particles nucleate droplets in eastern Atlantic clouds, *Geophys. Res. Lett.*, **36**.
- Tobías, A, L. Pérez, J. Díaz, C. Linares, J. Pey, A. Alastruey, and X. Querol, 2008: Short-term effects of particulate matter on total mortality during Saharan dust outbreaks: a case crossover analysis in Madrid (Spain). *Sci. Total Environ.*, **412-413**, 386-389.
- Touré N. E., A. Konaré, and S. Silué, 2012. "Intercontinental Transport and Climatic Impact of Saharan and Sahelian Dust," *Adv. Meteor.*, **2012**.
- Walsh, J. J., and K. A. Steidinger, 2001: Saharan dust and Florida red tides: The cyanophyte connection. *J. Geophys. Res.*, **106**, 11597–11612.
- Zhang, H., G. M. McFarquhar, S. M. Saleeby, and W. R. Cotton, 2007. "Impacts of Saharan dust as CCN on the evolution of an idealized tropical cyclone". *Geophys. Res. Lett.*, **34**.
- Zhao C, X Liu, LR Leung, and S Hagos, 2011: Radiative impact of mineral dust on monsoon precipitation variability over West Africa. *Atmos. Chem. Phys.*, **11(5)**, 1879-1893.